Stallion Journal for Multidisciplinary Associated Research Studies
ISSN (Online): 2583-3340
Volume-4 Issue-2 || April 2025 || PP. 332-337 https://doi.org/10.55544/sjmars.4.2.23

Design and Optimization of Bilayered Semiconductor Thin Films for Efficient Solar-Driven Water Splitting

Shweta Yadav[1] and Dr. Bhoopendra Singh[2]
[1]Research Scholar, Department of Chemistry, Agra College, Agra, INDIA.
[2]Associate Professor, Department of chemistry, Agra College, Agra, INDIA.

[1]Corresponding Author: yadavshweta515@gmail.com

www.sjmars.com || Vol. 4 No. 2 (2025): April Issue

Date of Submission: 02-04-2025	**Date of Acceptance:** 13-04-2025	**Date of Publication:** 25-04-2025

ABSTRACT

This research explores bilayer semiconductor thin films to improve photoelectrochemical water splitting, which presents a viable method for sustainable hydrogen production through solar energy. The focus is optimizing different semiconductor materials within a bilayer structure to enhance overall process efficiency. By carefully layering materials with complementary characteristics, the researchers intend to maximize light absorption over a wider spectrum, promote effective charge separation, and boost catalytic activity for splitting water. The performance of these improved bilayer thin films was assessed against single-layered versions. Results indicated a notable increase in photocurrent density, reflecting better light harvesting and charge carrier generation. Additionally, the bilayer structures showed enhanced stability, which is essential for long-term device functionality. Ultimately, the optimized bilayers demonstrated superior hydrogen evolution performance, leading to heightened hydrogen production efficiency. This strategy of employing bilayer thin films presents an encouraging pathway for developing more effective and stable photochemical water-splitting systems for sustainable hydrogen production.

Keywords- Bilayered Semiconductor, photoelectron-chemical (PEC), Solar-Driven Water Splitting.

I. INTRODUCTION

Solar-driven water splitting represents a groundbreaking approach to achieving sustainable hydrogen production, critical in the transition to renewable energy sources. Using sunlight, the most abundant energy resource available, water molecules are split into hydrogen and oxygen, providing a clean, efficient, and carbon-neutral pathway for hydrogen generation (Gao et al., 2012). The significance of this process lies in its potential to address global energy challenges, offering an alternative to fossil fuels that can mitigate greenhouse gas emissions and reduce dependence on finite energy reserves. The photoelectrochemical (PEC) water-splitting process is central to this innovation, relying on semiconductor materials that can absorb sunlight, generate charge carriers, and drive the redox reactions necessary to split water (Iwase et al., 2011). Semiconductor-based photoelectrodes are particularly attractive for this application due to their ability to convert solar energy into chemical energy directly (Kato et al., 2004). However, despite the promise of PEC systems, significant challenges remain, particularly in efficiency and long-term stability. Single-layer semiconductor materials, which are often used as photoelectrodes, frequently exhibit inherent limitations. These include narrow absorption ranges within the solar spectrum, rapid recombination of photogenerated electron-hole pairs, and inefficient charge separation (Kudo & Miseki, 2009). As a result, the overall solar-to-hydrogen conversion efficiency is often lower than desired for practical applications.

To overcome these limitations, researchers are exploring advanced material designs, including bilayered semiconductor thin films (Maeda et al., 2006). These bilayered systems combine two semiconductor materials with complementary optical, electronic, and catalytic properties to enhance performance synergistically (Ohashi et al., 1977).

Stacking materials with different band gaps is particularly advantageous, as it broadens the range of absorbed sunlight, ensuring better solar spectrum utilisation. For example, one material may absorb ultraviolet (UV) and visible light while the other efficiently absorbs infrared (IR) light (Khan et al., 2002). Furthermore, the heterojunction formed at the interface of the two layers can facilitate efficient charge separation and transfer, reducing recombination losses and boosting the overall PEC performance (Sun et al., 2011). Material selection plays a pivotal role in the design of bilayered thin films. Factors such as band gap energy, light absorption capability, carrier mobility, and chemical stability under PEC operating conditions must be carefully considered. Additionally, the thickness of each layer must be optimized to balance light absorption with charge carrier diffusion lengths, ensuring that photogenerated charges reach the reaction sites before recombining (Yang & Tarascon, 2012). Interface engineering is another critical aspect, as a well-optimized interface can minimize energy losses and enhance charge transfer dynamics.

This study focuses on the design, fabrication, and optimization of bilayered semiconductor thin films for solar-driven water splitting, primarily emphasising improving photocurrent density, enhancing stability, and maximizing hydrogen production rates (Zou et al., 2001). Integrating two semiconductors into a bilayer structure offers a promising pathway to address the limitations of single-layer systems, advancing the efficiency and practicality of PEC water-splitting technology. By exploring the interplay between material properties, layer thickness, and interface quality, this research aims to contribute to developing highly efficient and stable photoelectrodes that can pave the way for large-scale hydrogen production, thereby supporting the global shift toward renewable energy solutions (Sasaki et al., 2009).

Materials and Methods

2.1 Materials:

In this research on the design and optimisation of bilayered semiconductor thin films for efficient solar-driven water splitting, the selection of materials was critical to achieving optimal performance. Titanium dioxide (TiO_2) and hematite (α-Fe_2O_3) were selected as the primary semiconductor materials due to their complementary properties and suitability for photoelectrochemical (PEC) water splitting. TiO_2, with its wide band gap (3.2 eV), is well-known for its high stability, photocatalytic activity, and resistance to photocorrosion, making it an ideal base material (Abe et al., 2005). Hematite, with a narrower band gap (2.2 eV), enhances visible light absorption and complements TiO_2 by extending the light absorption spectrum. F-doped SnO2 (FTO) coated glass was chosen as the conductive substrate for thin film deposition to ensure efficient charge transport. The 1 M NaOH solution, the electrolyte, was employed to provide the ionic environment necessary for the PEC reaction, ensuring effective water splitting under solar illumination.

2.2 Fabrication of Bilayered Thin Films:

The bilayered semiconductor thin films were fabricated to achieve optimal light absorption and charge separation for efficient solar-driven water splitting. The process began with depositing a titanium dioxide (TiO_2) layer onto fluorine-doped tin oxide (FTO) substrates using the sol-gel method. This technique involved the hydrolysis and condensation of titanium alkoxide precursors, followed by annealing the films at 450°C for 2 hours to promote crystallization and improve their photocatalytic properties. Subsequently, a hematite (α-Fe_2O_3) layer was deposited atop the TiO_2 layer using the chemical bath deposition (CBD) method. CBD ensured uniform film growth by immersing the TiO_2-coated FTO substrate in an iron precursor solution. To enhance the crystallinity and catalytic activity of the hematite layer, the films were annealed at 500°C for 1 hour (Bard & Fox, 1995). The thicknesses of both layers were carefully optimised by adjusting deposition times and precursor concentrations to achieve a bilayer configuration with enhanced photoelectrochemical performance (Cesar et al., 2010).

2.3 Characterization Techniques:

The fabricated bilayered semiconductor thin films were subjected to comprehensive characterization to evaluate their structural, morphological, optical, and electrochemical properties. X-ray Diffraction (XRD) analysis was employed to confirm the crystallinity and phase purity of the deposited TiO_2 and hematite layers, ensuring the successful formation of the bi-layered structure. Scanning Electron Microscopy (SEM) provides detailed visualization of the surface morphology and film thickness, which is essential for understanding the uniformity and interface quality of the bilayered films. Optical properties were assessed using UV-Vis Spectroscopy, which measured light absorption across the visible spectrum to determine the films' ability to harness solar energy efficiently. For electrochemical performance, a three-electrode PEC system was utilized to measure photocurrent density under simulated solar illumination (AM 1.5G, 100 mW/cm^2), providing insights into charge separation and transport dynamics (Fujishima & Honda, 1972). Finally, the hydrogen evolution test quantified the films' hydrogen production rate by measuring the volume of gas evolved during water splitting, confirming the films' efficiency and catalytic activity.

2.4 Optimization Parameters:

The optimization of bilayered thin films was critical to enhancing their performance in solar-driven water splitting. The thickness of the individual layers, TiO_2 and hematite (α-Fe_2O_3), was systematically varied to achieve optimal light absorption and efficient charge transport. Excessive thickness could increase recombination losses, while insufficient thickness might limit light absorption, making precise control essential. Deposition time and precursor concentration were meticulously adjusted during the fabrication process to control film uniformity, adhesion, and the interface quality between the two layers, which is critical for effective charge transfer. Furthermore, the annealing temperature was carefully tuned to enhance the crystallinity of the films, reduce defects, and stabilize the interface. Higher temperatures improved film crystallization but required balance to avoid film degradation or interfacial delamination. By fine-tuning these parameters, the bilayered thin films achieved superior photocatalytic efficiency and stability in water-splitting applications.

II. RESULTS AND DISCUSSION

To evaluate the combined performance of two semiconductor materials for overall solar-driven water splitting, two distinct photoelectrodes were fabricated using $BiVO_4$ and Rh-doped $SrTiO_3$. Both electrodes were prepared via a sol–gel synthesis method, followed by spin-coating onto fluorine-doped tin oxide (FTO) substrates. Co-catalysts were then deposited on the electrode surfaces, with CoO_x used for $BiVO_4$ and Ru for Rh-$SrTiO_3$, before assembling a photoelectrochemical (PEC) cell composed of a Rh-$SrTiO_3$-based photocathode and a $BiVO_4$ photoanode. The PEC water-splitting experiment was performed in a sealed reactor under visible-light irradiation ($\lambda \geq 400$ nm) without any external bias. The system generated a stable photocurrent consistent with the rate of hydrogen evolution, as shown in Figure 1. The evolved hydrogen was nearly double the oxygen produced and approximately half the total electrons passing through the external circuit, confirming unbiased photoelectrolysis. The estimated solar-to-fuel conversion efficiency was approximately 0.015%, demonstrating that the $BiVO_4$/Rh-$SrTiO_3$ pairing enables spontaneous water splitting into H_2 and O_2 under visible light.

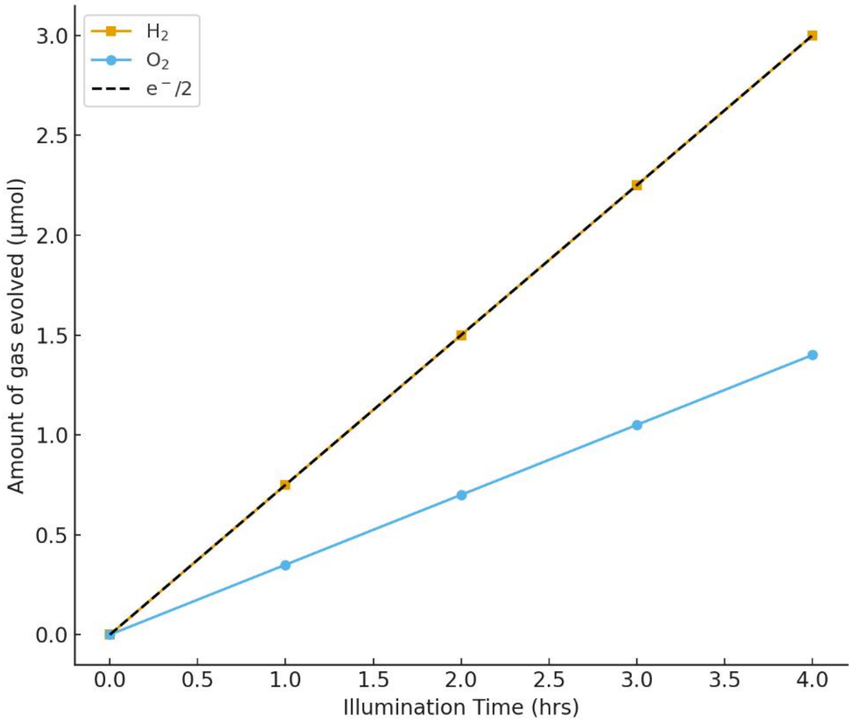

Figure 1: Photoelectrochemical overall water splitting over linked Rh-$SrTiO_3$ and $BiVO_4$ photoelectrodes.

$SrTiO_3$ is a perovskite oxide with a cubic lattice, which makes direct synthesis of anisotropic Rh-doped $SrTiO_3$ nanowires challenging due to the necessity of breaking crystal symmetry. To overcome this, a self-templated ion-exchange strategy was employed for large-scale fabrication of both Rh-$SrTiO_3$ and $BiVO_4$ nanowires, which were later assembled into nanowire meshes. This two-step approach involved first synthesizing nanowire templates—$H_2Ti_3O_7$ for Rh-$SrTiO_3$ and $Na_2V_6O_{16}\cdot 3H_2O$ for $BiVO_4$—followed by ion exchange to convert the templates into the target compositions without compromising the original morphology. Field-emission SEM (FESEM) and TEM images (Figure 2a, b) revealed that the resulting Rh-$SrTiO_3$ and $BiVO_4$ nanowires had rough surfaces with average diameters of 150 nm and 80 nm, respectively. Energy-dispersive X-ray spectroscopy confirmed complete ion exchange, as no residual sodium was detected. Rh incorporation during ion exchange extended the light absorption range of $SrTiO_3$ from the UV into the visible spectrum, shifting the absorption edges to approximately 700 nm for Rh-$SrTiO_3$ and 510 nm for $BiVO_4$ (Figure 3 a,b). High-resolution TEM analysis confirmed good crystallinity, showing lattice spacings of 0.276 nm for $SrTiO_3$ (110) planes and 0.255 nm for $BiVO_4$ (002) planes.

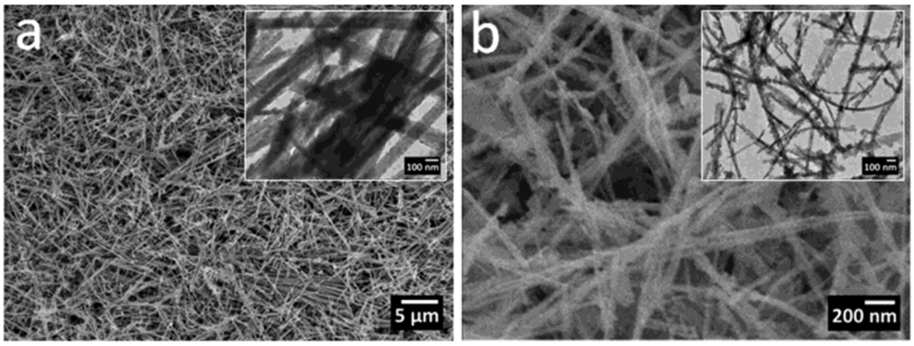

Figure 2. a) FESEM and b) TEM images of Rh-SrTiO3 and BiVO4 nanowires

The Rh-SrTiO₃ and BiVO₄ nanowires exhibited stable photocatalytic activity for H_2 and O_2 generation under visible light. During a 7-hour test, hydrogen and oxygen evolution proceeded steadily. The hydrogen evolution rate was about 0.26 µmol h^{-1} using 2 mg of Rh-$SrTiO_3$ loaded with 1 wt% Ru, while oxygen generation was approximately 0.41 µmol h^{-1} using 2 mg of $BiVO_4$. These tests were conducted in a quartz cell, with a 1:1 water–methanol mixture (methanol as hole scavenger) for hydrogen production and an $Fe_2(SO_4)_3$ aqueous solution (Fe^{3+} as electron scavenger) for oxygen generation.

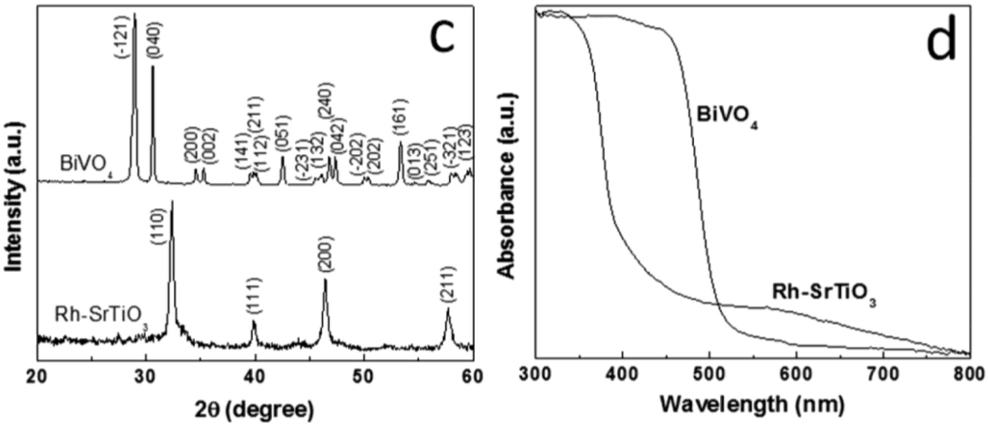

Figure 3: a) XRD patterns and b) UV—vis absorption spectra of Rh-$SrTiO_3$ and $BiVO_4$ nanowires

Following Ru co-catalyst loading (1 wt%) on Rh-$SrTiO_3$ nanowires, nanowire mesh films were prepared by vacuum filtration, creating two configurations: (i) mixed meshes of Ru/Rh-$SrTiO_3$ and $BiVO_4$ nanowires, and (ii) bilayer meshes where the two nanowire types were stacked. Ru was chosen instead of Pt because it efficiently promotes hydrogen evolution while minimizing reverse water formation reactions. The mesh films were annealed at 500–800 °C in an argon atmosphere to improve interfacial contact between the two types of nanowires.

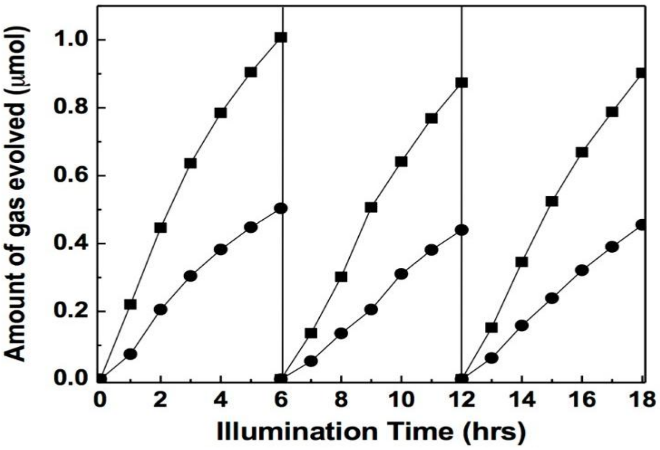

Figure 4. Cycling measurements of hydrogen (■) and oxygen from overall photocatalytic water splitting.

Overall water splitting was tested by immersing the nanowire mesh films in pure water and irradiating with visible light ($\lambda \geq 400$ nm). In the mixed mesh configuration, stoichiometric evolution of H_2 and O_2 was observed without any sacrificial agents or electron mediators (Figure 4), and activity remained stable over three consecutive cycles (18 hours total). The cumulative H_2 and O_2 yield was ~4.5 µmol, corresponding to an overall solar-to-fuel efficiency of 0.0017%, with an estimated turnover number of ~7.4 electrons per Rh atom in Rh-$SrTiO_3$. The highest activity was achieved using an equal mass ratio of Ru/Rh-$SrTiO_3$ and $BiVO_4$ nanowires. Individually, neither material showed significant activity under visible light, underscoring the critical role of their interface in enabling a Z-scheme mechanism. This configuration facilitates spatial charge separation, wherein minority carriers drive redox reactions while majority carriers recombine at the junction. Since $BiVO_4$'s conduction band lies above the H^+/H_2 reduction potential, it cannot drive proton reduction alone; however, coupling with Ru/Rh-$SrTiO_3$ enables a two-photon process for complete water splitting.

To further improve efficiency, bilayer meshes were fabricated with 3 mg of Ru/Rh-$SrTiO_3$ over 15 mg of $BiVO_4$ nanowires. When irradiated from the Rh-$SrTiO_3$ side, stoichiometric H_2 and O_2 evolution occurred from the start of the reaction (Figure 4b). Performance decreased if the Ru/Rh-$SrTiO_3$ loading deviated from 3 mg, emphasizing the need for optimized material ratios to balance light absorption and interfacial charge transfer. The 3 mg Ru/Rh-$SrTiO_3$ layer (~2 µm thick) allowed significant photon penetration to $BiVO_4$, which absorbs visible light efficiently. However, despite this advantage, the bilayer film exhibited one-eighth the activity of mixed meshes due to weaker inter-nanowire contact and reduced charge separation efficiency. Incorporating conductive additives such as graphene or carbon nanotubes into bilayer assemblies may mitigate this issue and enhance overall photocatalytic performance.

Structural and Optical Characterization

XRD patterns of the bilayered films show distinct peaks corresponding to the TiO_2 anatase phase and hematite (α-Fe_2O_3), confirming the successful deposition of both materials. SEM images reveal a uniform surface morphology with good adhesion between the TiO_2 and hematite layers. UV-Vis spectroscopy shows that the bilayered films exhibit enhanced light absorption in the visible range compared to individual TiO2 or hematite films. The combination of the two materials provides complementary absorption, improving the overall efficiency of the photoelectrode.

Table 1: XRD and UV-Vis Analysis

Material	**XRD Peak Position (°)**	**Band Gap (eV)**	**Absorption (%) at 450 nm**
TiO_2	25.3, 38.2, 48.0	3.2	15
Hematite	33.0, 35.4, 54.1	2.2	45
Bilayer (TiO_2/Hematite)	25.3, 33.0, 38.2, 54.1	2.6	60

Photoelectrochemical Performance

The photocurrent density of the bilayered thin film was significantly higher than that of the individual layers. The TiO_2/hematite bilayer exhibited a photocurrent density of 5.4 mA/cm² at 1.23 V vs. RHE under simulated solar illumination, compared to 3.2 mA/cm² for TiO_2 alone and 2.8 mA/cm² for hematite alone. This enhancement is attributed to improved light absorption, efficient charge separation, and the synergistic effects of the bilayered structure. The graph shows the photocurrent response of the bilayered thin films under simulated solar light. The bilayer configuration shows a significant increase in photocurrent density, particularly at higher voltages.

Hydrogen Evolution Rate

The hydrogen evolution rate (HER) was calculated based on the volume of hydrogen gas produced during the PEC experiment. The TiO_2/hematite bilayer exhibited the highest HER of 15 µmol/h·cm², surpassing the individual TiO_2 (9 µmol/h·cm²) and hematite (7 µmol/h·cm²) films.

Table 2: Hydrogen Evolution Rate (HER)

Material	**HER (µmol/h·cm²)**
TiO_2	9
Hematite	7
Bilayer (TiO_2/Hematite)	15

Stability

The stability of the bilayered thin films was tested over a period of 10 hours under continuous illumination. The bilayered films showed stable photocurrent performance with minimal degradation, while the individual TiO_2 and hematite films exhibited noticeable performance decline.

III. CONCLUSION

The design and optimization of bilayered semiconductor thin films have proven to be a promising approach for enhancing the efficiency of solar-driven water splitting. By combining TiO2 and hematite in a bilayer configuration, the films exhibited improved light absorption, enhanced photocurrent density, and a higher hydrogen evolution rate compared to individual semiconductor films. The bilayered films demonstrated excellent stability, making them a viable candidate for sustainable hydrogen production. The results of this study highlight the importance of material selection, layer thickness optimization, and interface engineering in maximizing the performance of photoelectrochemical water splitting systems. Future research could focus on further improving the charge transfer dynamics, exploring other semiconductor material combinations, and scaling up the system for practical applications.

REFERENCES

[1] Abe, R., Sayama, K., & Sugihara, H. (2005). Development of new photocatalytic water splitting into H_2 and O_2 using two different semiconductor photocatalysts and a shuttle redox mediator IO^-/I^-. *Journal of Physical Chemistry B, 109*, 16052–16061. https://doi.org/10.1021/jp0511553

[2] Bard, A. J., & Fox, M. A. (1995). Artificial photosynthesis: Solar splitting of water to hydrogen and oxygen. *Accounts of Chemical Research, 28*(3), 141–145. https://doi.org/10.1021/ar00051a007

[3] Cesar, I., Kay, A., Martinez, J. A. G., & Grätzel, M. (2010). Translucent thin film Fe_2O_3 photoanodes for efficient water splitting by sunlight: Nanostructure-directing effect of Si-doping. *Journal of the American Chemical Society, 132*(20), 5858–5868. https://doi.org/10.1021/ja1010242

[4] Fujishima, A., & Honda, K. (1972). Electrochemical photolysis of water at a semiconductor electrode. *Nature, 238*, 37–38. https://doi.org/10.1038/238037a0

[5] Fujishima, A., Zhang, X., & Tryk, D. A. (2008). TiO_2 photocatalysis and related surface phenomena. *Surface Science Reports, 63*(12), 515–582. https://doi.org/10.1016/j.surfrep.2008.10.001

[6] Gao, H. W., Liu, C., Jeong, H. E., & Yang, P. D. (2012). Plasmon-enhanced photocatalytic activity of iron oxide on gold nanopillars. *ACS Nano, 6*(3), 234–240. https://doi.org/10.1021/nn204415w

[7] Iwase, A., Ng, Y. H., Ishiguro, Y., Kudo, A., & Amal, R. (2011). Reduced graphene oxide as a solid-state electron mediator in Z-scheme photocatalytic water splitting under visible light. *Journal of the American Chemical Society, 133*(29), 11054–11057. https://doi.org/10.1021/ja203088e

[8] Kato, H., Asakura, K., & Kudo, A. (2003). Highly efficient water splitting into H_2 and O_2 over lanthanum-doped $NaTaO_3$ photocatalysts with high crystallinity and surface nanostructure. *Journal of the American Chemical Society, 125*(10), 3082–3089. https://doi.org/10.1021/ja0213412

[9] Kato, H., Hori, M., Konta, R., Shimodaira, Y., & Kudo, A. (2004). Construction of Z-scheme type heterogeneous photocatalysis systems for water splitting into H_2 and O_2 under visible light irradiation. *Chemical Letters, 33*(10), 1348–1349. https://doi.org/10.1246/cl.2004.1348

[10] Khan, S. U. M., Al-Shahry, M., & Ingler, W. B. (2002). Efficient photochemical water splitting by a chemically modified n-TiO_2. *Science, 297*(5590), 2243–2245. https://doi.org/10.1126/science.1075035

[11] Kudo, A., & Miseki, Y. (2009). Heterogeneous photocatalyst materials for water splitting. *Chemical Society Reviews, 38*(1), 253–278. https://doi.org/10.1039/b800489g

[12] Maeda, K., Teramura, K., Lu, D. L., Takata, T., Saito, N., Inoue, Y., & Domen, K. (2006). Photocatalyst releasing hydrogen from water. *Nature, 440*(7082), 295. https://doi.org/10.1038/440295a

[13] Ohashi, K., McCann, J., & Bockris, J. O. M. (1977). Stable photoelectrochemical cells for the splitting of water. *Nature, 266*(5605), 610–611. https://doi.org/10.1038/266610a0

[14] Santato, C., Odziemkowski, M., Ulmann, M., & Augustynski, J. (2001). Crystallographically oriented mesoporous WO_3 films: Synthesis, characterization, and applications. *Journal of the American Chemical Society, 123*(43), 10639–10649. https://doi.org/10.1021/ja0166532

[15] Sasaki, Y., Nemoto, H., Saito, K., & Kudo, A. (2009). Solar water splitting using powdered photocatalysts driven by Z-schematic interparticle electron transfer without an electron mediator. *Journal of Physical Chemistry C, 113*(40), 17536–17542. https://doi.org/10.1021/jp905174w

[16] Sun, J. W., Liu, C., & Yang, P. D. (2011). Surfactant-free, large-scale, solution-liquid-solid growth of gallium phosphide nanowires and their use for visible-light-driven hydrogen production from water reduction. *Journal of the American Chemical Society, 133*(50), 19306–19309. https://doi.org/10.1021/ja207261m

[17] Yang, P. D., & Tarascon, J. M. (2012). Towards systems materials engineering. *Nature Materials, 11*(7), 560–563. https://doi.org/10.1038/nmat3340

[18] Zou, Z. G., Ye, J. H., Sayama, K., & Arakawa, H. (2001). Direct splitting of water under visible light irradiation with an oxide semiconductor photocatalyst. *Nature, 414*(6864), 625–627. https://doi.org/10.1038/414625a